




Article

N-Oleoyl Sarcosine as an Engine Oil Friction Modifier, Part 2: Elucidation of Friction-Reducing Mechanism at Room Temperature Focusing on Contribution of NOS in NOS+ZDDP Mixture

Wei qi Shen¹⁾, Dongjiang Han²⁾, Tomoko Hirayama ^{1)*}, Naoki Yamashita¹⁾,
Tadashi Oshio³⁾, Hideo Tsuneoka³⁾, Kazuo Tagawa³⁾ and Kazuhiro Yagishita³⁾

¹⁾Department of Mechanical Engineering and Science, Graduate School of Engineering, Kyoto University,
Katsura, Nishikyo-ku, Kyoto 615-8540, Japan

²⁾Institute of Engineering Thermophysics, Chinese Academy of Sciences,
No.11 North 4th Ring West Rd., Beijing 100190, PR China

³⁾Lubricants R&D Dept., ENEOS Corporation,
8 Chidoricho, Naka-ku, Yokohama 231-0815, Japan

*Corresponding author: Tomoko Hirayama (tomoko@me.kyoto-u.ac.jp)

Manuscript received 06 July 2022; accepted 02 September 2022; published 30 September 2022

Abstract

The tribological properties of a mixture of a commercial organic friction modifier, N-oleoyl sarcosine (NOS), and a commercial anti-wear additive, zinc dialkyldithiophosphate (ZDDP), were investigated. The results suggest a synergistic effect between these two additives, resulting in a mixture that exhibited the lowest and most stable friction coefficient as well as the smallest wear area. X-ray photoelectron spectroscopy was performed to investigate the chemical composition of the tribo-films formed using this mixture. The results suggest that the tribo-films lacked S as well as PO_4^{3-} species. They also suggest that ZDDP mitigates degradation of the NOS, and improve the tribo-film durability thus improving anti-wear/friction-reducing performance. These results elucidate the synergistic friction-reducing tribological mechanism of the NOS+ZDDP mixture.

Keywords

ZDDP, organic friction modifiers, boundary lubrication, XPS, ball on disc

1 Introduction

The usage of mixed engine oil additives, especially the synergy between zinc dialkyldithiophosphate (ZDDP) and various organic friction modifiers (OFMs), has been investigated over the past decade due to the urgent need to improve the lubricity of low-viscosity engine oil under boundary lubrication conditions. Among these OFMs, the tribological behavior of glycerol monooleate (GMO), a widely commercialized OFM, in combination with ZDDP has been largely clarified. However, the boundary-friction reduction and wear resistance provided by the GMO+ZDDP additive mixture is no better than those of GMO alone and ZDDP alone [1–6]. Mixtures of ZDDP and OFMs containing amino groups have also been investigated [4, 7–9]. Some, such as the mixture of ZDDP and the primary monoamine, have exhibited synergistic effects in friction reduction and wear resistance, but the effects depend on the amine/ZDDP molar ratio [8]. Moreover, studies suggest that aminic FMs can remove or even damage the ZDDP tribo-film, a

negative factor in wear resistance [10–13].

In a companion paper, the authors introduced the usage of N-oleoyl sarcosine (NOS), consisting of an oleoyl tail, a carboxyl group, and an amide group. The tribological performance of NOS additive alone and combined with ZDDP under boundary lubrication conditions was investigated using a ball-on-disk tribometer at a representative engine operating temperature. The NOS alone was effective in reducing friction and exhibited the lowest friction coefficient among the four lubricating oils tested for the first 30 minutes. Over a longer testing time or with a heavier load, its tribological performance was inferior to that of the NOS+ZDDP mixture. The friction coefficient and the wear diameter increased noticeably. In contrast, the NOS+ZDDP mixture exhibited a stable friction coefficient under all loads, and the wear diameter stayed about the same. The results of the surface analysis to explain the synergy between NOS and ZDDP suggest that ZDDP mitigates NOS degradation, which might be the reason for the increased friction with NOS alone. Furthermore, NOS may reduce the contact severity, preventing

S formation in the tribo-film. Moreover, its strong adsorption due to chelate formation between the sarcosine head and metal may also prevent the adsorption of ZDDP decomposition products.

While much was clarified in the companion paper, the synergistic mechanism remained unclarified. The results presented demonstrate that the boundary tribo-film formation process with each lubricating oil is important in friction reduction. More specific information about the tribo-film formation process is necessary to understand the friction-reduction with NOS additive alone and with the NOS+ZDDP additive mixture. In addition to elucidating the tribo-film formation process, chemical composition analysis would help clarify the synergistic mechanism. Although the results of energy dispersive X-ray spectroscopy (EDX) were reported in the companion paper, a more precise analysis of the outermost surface of the tribo-films is necessary as the outermost surface greatly affects tribological behavior. In addition to the element composition, the chemical state of the tribo-films needs to be clarified. The current study was conducted at room temperature so that the ZDDP would be less active, enabling the authors to focus on the contribution of NOS in tribo-film formation. Moreover, as tribological severity is lower at room temperature than at an engine operating temperature, the tribo-film formation process can be clarified. X-ray spectroscopy (XPS) studies were conducted to investigate the chemical state of the outermost tribo-film surface. The results are discussed together with those presented in the companion paper in order to elucidate the synergistic mechanism between NOS and ZDDP.

2 Experimental materials and methods

2.1 Tribo-tests

The SUJ2 disks (15×15×4 mm) and balls (3/16-inch diameter) used in this study were the same as those described in the companion paper. Tribo-tests were carried out using a ball-on-disk setup (FPR-2100, RHESCA, Japan, cf. Fig. 1). The test conditions are listed in Table 1. The linear reciprocating tribo-tests were performed under boundary lubrication

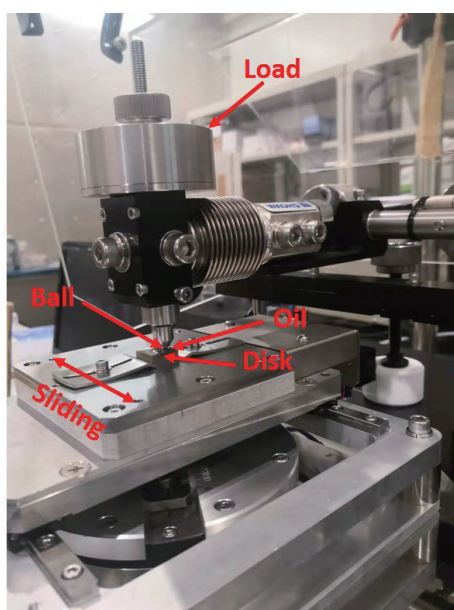


Fig. 1 Ball-on-disk set-up used for tribo-tests

Table 1 Tribo-test conditions

Parameter	Values
Frequency (Hz)	1
Sliding speed (mm/s)	10
Stroke length (mm)	5
Normal load (N)	1, 3, 5
Test duration (s)	1800
Ball diameter (in.)	3/16
Maximum pressure (MPa)	764, 1102, 1306
Average pressure (MPa)	509, 734, 871
Temperature (°C)	25

conditions (60- μ L disk lubrication). Each test was repeated three times to obtain the average coefficient of friction. The averages over the last 200 of the 1800 cycles were averaged to obtain the steady-stage friction coefficient. After the test, the worn balls and disks were cleaned with acetone and hexane respectively in an ultrasonic bath, and their worn states were imaged microscopically at the same magnification. The worn disks were then marked for XPS analysis.

The lubricating oils were the same as those described in the companion paper. Their compositions are listed in Table 2.

2.2 Surface analyses (Microscopy, XPS)

An ultra-high-magnification USB microscope (NSH130CS-R, SHODENSHA, Inc., Japan) was used to evaluate the wear condition of the balls and disks after the tribo-tests. The widths of the wear tracks on the disks and the wear areas on the balls were measured for anti-wear evaluation.

XPS analyses were performed using a PHI 5000 VersaProbe2 X-ray Photoelectron Spectroscopy (ULVAC Equipment Sales, Inc., Japan). The excitation source was a monochromatized Al K α X-ray beam (100- μ m diameter; 117.4-eV pass energy). The worn disks after the tribo-tests at 5 N were analyzed. Analysis points inside and outside the wear areas were selected using secondary X-ray images of the substrate surfaces. An example image is shown in Fig. 2. Data processing was performed using CasaXPS software (version 2.3.24, Casa Software Ltd., UK). The spectra were fitted using the product of Gaussian and Lorentzian functions after subtracting a Shirley background.

Table 2 Lubricating oils

Lubricating oil	Additive
PAO (poly- α -olefin)	none
PAO+ZDDP	ZDDP (700 ppm P)
PAO+NOS	NOS (0.3 mass%)
PAO+ZDDP+NOS	NOS (0.3 mass%) and ZDDP (700 ppm P)

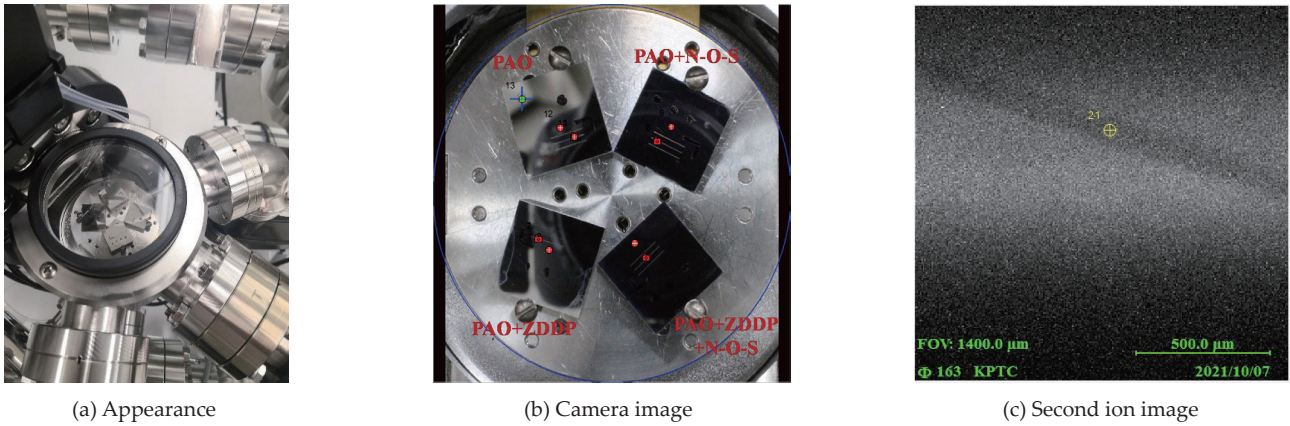


Fig. 2 XPS analysis

3 Results and discussion

3.1 Tribological behavior

3.1.1 Friction coefficient

The friction coefficients under 1, 3, and 5 N loads are shown in Figs. 3a, b, and c, respectively. The enlarged view for the first 600 cycles under a 5 N load shown in Fig. 3d clearly shows the changes in the friction coefficients during the running-in cycles

for the three additive mixtures.

The trends in the friction coefficient were similar for the three additive mixtures under all applied loads. The friction coefficient with PAO+NOS was the lowest over the first several hundred cycles and then slightly exceeded that with PAO+ZDDP+NOS and stabilized. The friction coefficient with the ZDDP additive initially increased, probably due to ZDDP tribo-film formation. The trend with PAO+ZDDP+NOS was

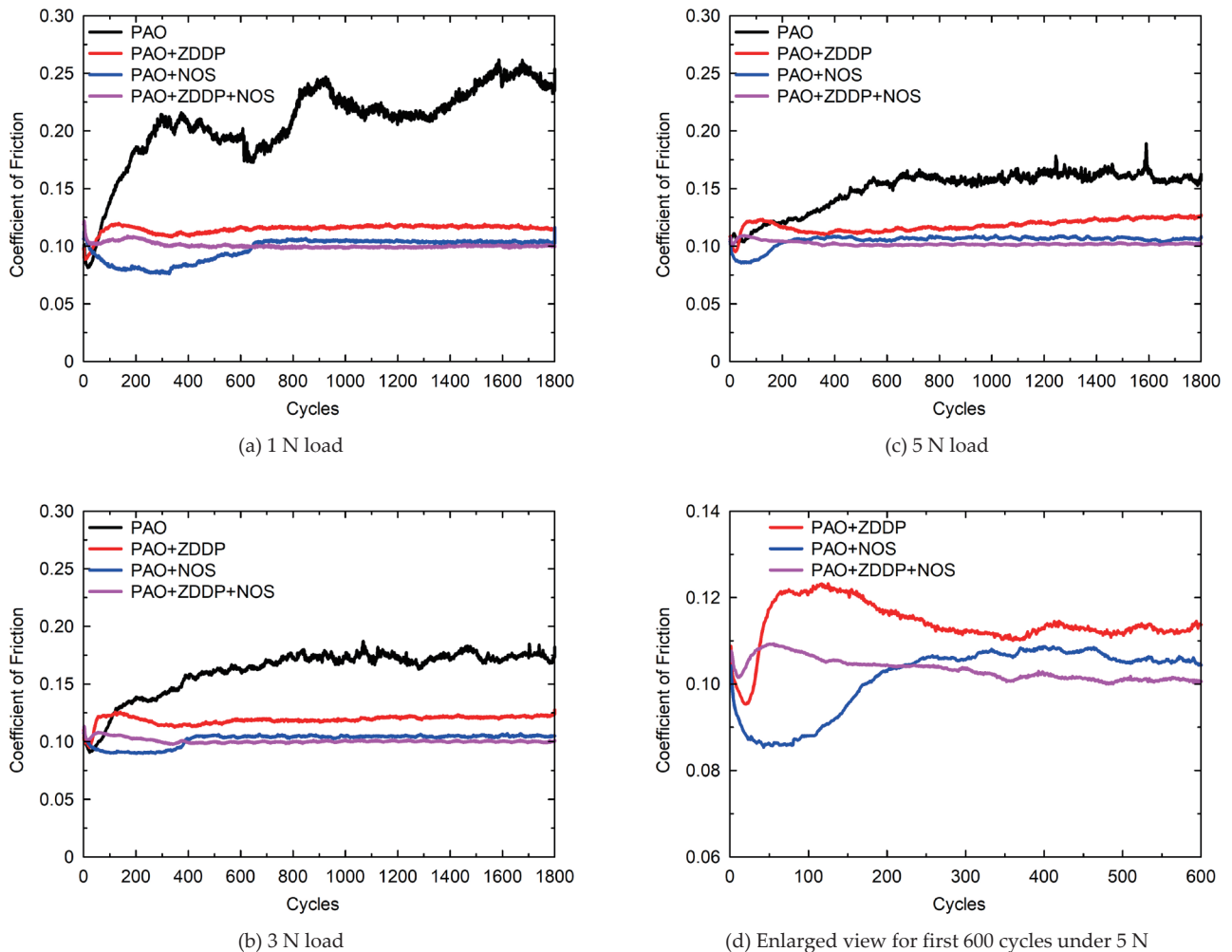


Fig. 3 Friction coefficient curves over 1800 cycles under different loads

similar to that of PAO+ZDDP but was more stable from the first cycle. Another similarity was that the friction coefficient stabilized more quickly as the applied load was increased. With PAO+NOS, it decreased to 0.078 after about 300 cycles and increased to 0.104 after about 660 cycles, and stabilized at 1 N (Fig. 3a). It took only 430 cycles to stabilize at 3 N (Fig. 3b) and 260 cycles at 5 N (Fig. 3c). The trend was the same with PAO+ZDDP and PAO+ZDDP+NOS, especially at 5 N (Fig. 3c); with PAO+ZDDP+NOS, it stabilized after only several ten cycles at 5 N. This suggests that a heavier load promotes tribo-film formation, leading to stable friction behavior.

Moreover, with PAO+ZDDP+NOS, friction behavior was similar to but more stable than that of PAO+ZDDP during the first several hundred cycles. As shown in Fig. 3d, both additive mixtures exhibited a decrease-increase-decrease friction behavior. However, with PAO+ZDDP, it took 20 cycles for friction to start increasing, whereas, with PAO+ZDDP+NOS, it took only 10 cycles. On the other hand, with PAO+ZDDP, the maximum friction coefficient reached 0.123, whereas, with PAO+ZDDP+NOS, it reached only 0.109. After the friction coefficient reached a maximum with PAO+ZDDP+NOS, it stabilized after 400 cycles. In contrast, the friction coefficient with PAO+ZDDP decreased to 0.11 after 350 cycles and then started to increase, which is clearly evident in Fig. 3c. These differences in trend between ZDDP and NOS/NOS+ZDDP suggest that the NOS in the mixture contributed more to friction behavior, at least under the 5 N load.

The results shown in Fig. 3 are similar to those at 100°C presented in the companion paper. In particular, the ordering of the friction coefficients with NOS alone and with NOS+ZDDP was the same. The friction coefficient was initially the lowest with NOS; it then increased and exceeded that of NOS+ZDDP. There was a difference, however, in the time taken. It took only several hundred cycles at 25°C, whereas it took about 2000 cycles at 100°C. A higher temperature enhances the adsorption of OFMs [14], so the NOS can likely help form a denser film at 100°C, which prolongs the durability of the adsorption film.

The steady friction coefficients under different loads for each lubricating oil are shown in Fig. 4. The friction coefficients for the last 200 cycles were averaged to obtain a steady friction

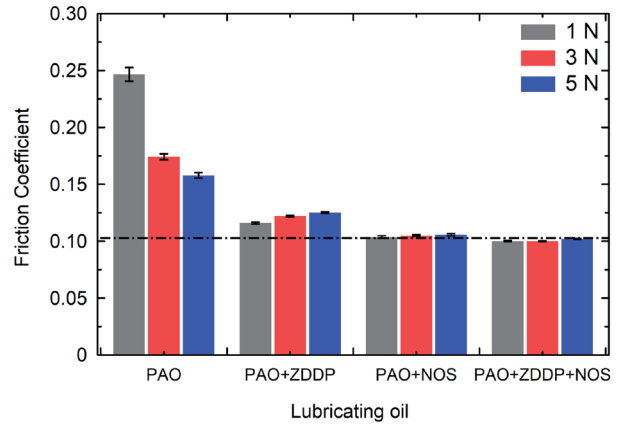


Fig. 4 Steady friction coefficients with different lubricating oils

coefficient. The black dotted line in Fig. 4 represents the steady friction coefficient of PAO+ZDDP+NOS at 5 N as a reference. As the load increased, the steady friction coefficients gradually decreased for PAO. In contrast, the steady coefficients of friction increased slightly with the increase in the load for all the lubricating oils with additives. This does not match the results presented in the companion paper: after 1800 sliding cycles, the NOS additive alone exhibited a much lower friction coefficient than that of the NOS+ZDDP additive mixture. However, the current results agree well with those for longer testing/heavier load conditions presented in the companion paper. This may have been due to degradation of the NOS adsorption film, which will be discussed later.

3.1.2 Wear state analysis

The worn state of balls and disks after 1800 sliding cycles under 5 N load conditions were imaged, as shown in Figs. 5a, b, c, and d refer to the ball and disk pair lubricated with PAO, PAO+ZDDP, PAO+NOS, and PAO+ZDDP+NOS. The arrow direction shown in Fig. 5a indicates the sliding direction. The wear diameter of the balls is consistent with the wear width of the disks.

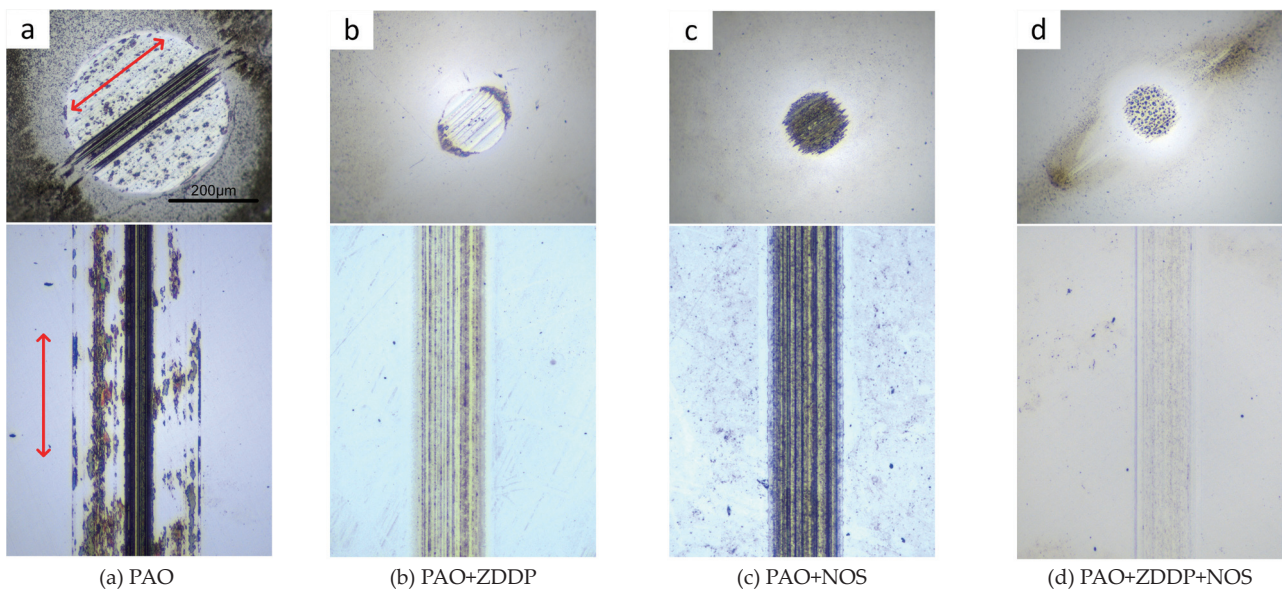


Fig. 5 Microscopically obtained wear states for 5 N after 1800 cycles

PAO exhibited an adhesive-wear-like feature. As shown in Fig. 5a, some of the shed particles were attached to the ball surface even in the noncontact area. This is because the contact surface was in direct contact with each other, so the adhesion points were sheared and transferred to the ball surface during sliding. At the same time, since the base oil could not provide sufficient protection to the friction surface, ravine-like scars can be clearly seen in the contact area. The width of the scars increased with the load. The addition of the additives improved the wear resistance noticeably. As shown in Fig. 5b, with PAO+ZDDP, the tribo-film on the ball had ravine-like wear scars, but the wear was clearly less than with PAO alone. With PAO+NOS (Fig. 5c), the tribo-film was relatively uniform over the entire wear area, and ravine-like wear features are evident. With PAO+ZDDP+NOS (Fig. 5d), only point-like wear characteristics rather than ravine-like wear are evident. The point-like wear characteristics may be the reason for the synergistic effects in friction reduction and wear resistance. On the disks, extremely light wear is evident for PAO+ZDDP+NOS (Fig. 5d), and similar levels of wear are evident for PAO+ZDDP (Fig. 5b) and PAO+NOS (Fig. 5c).

Figure 6 shows the relative wear diameters of the balls with different lubricating oils and under different load conditions. The relative wear diameters were calculated using that for PAO at 5 N as 1.0. As the load was increased from 1 to 5 N, the wear diameter increased. The wear diameter for PAO+ZDDP+NOS was the smallest at each load, which agrees with it having the lowest friction coefficient. The increase in the wear diameter when the load was increased from 3 to 5 N was the largest for PAO and the smallest for PAO+ZDDP+NOS. These results agree well with those presented in the companion paper: the wear diameter with the NOS+ZDDP mixture stayed about the same when the load was increased from 3 to 5 N. The wear diameter remained unchanged with additional sliding cycles. These results suggest that the NOS+ZDDP additive mixture promotes positive wear resistance at both 25 and 100°C.

3.1.3 Tribo-film formation process

The friction coefficients for the first 600 cycles at 5 N are shown in Fig. 7. Each lubricating oil exhibited a different behavior over the 600 cycles. The PAO+NOS one exhibited the lowest friction coefficient over the first 200 cycles, which suggests that a sufficient adsorbed layer of NOS between the ball and the disk effectively reduces friction. The friction coefficient subsequently increased. The reason for the increase

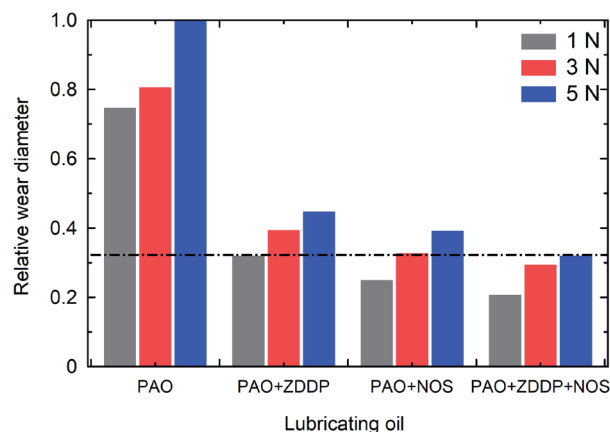


Fig. 6 Relative wear diameters with different lubricating oils after 1800 cycles

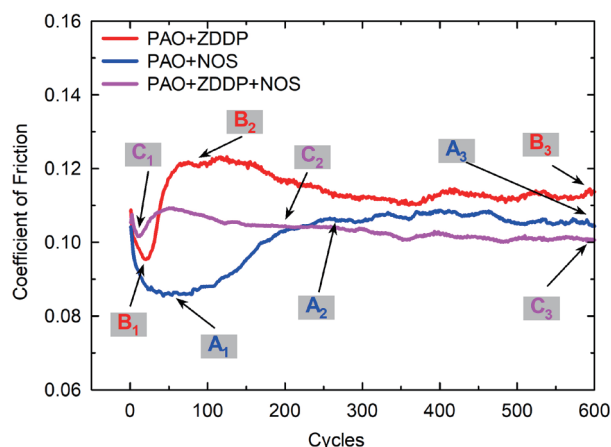


Fig. 7 Friction coefficients for first 600 cycles at 5 N

will be discussed below. The PAO+ZDDP oil exhibited the highest friction coefficient after 40 cycles. The friction coefficient increase after 20 cycles may correlate with ZDDP tribo-film formation. The PAO+ZDDP+NOS oil exhibited the highest friction coefficient over the first 40 cycles but did not change drastically and became the lowest after 200 cycles.

The contact areas of the balls at each point on the friction coefficient curves where the coefficient became stable were imaged to clarify the relationship between the tribo-film morphology and the friction coefficient. For PAO+NOS, these points were at the 60th, 200th, and 600th cycle, marked as A₁, A₂, and A₃, respectively. For PAO+ZDDP, they were at the 20th, 75th, and 600th cycle (B₁, B₂, and B₃); for PAO+ZDDP+NOS, they were at the 10th, 200th, and 600th cycle (C₁, C₂, and C₃).

The results are shown in Figs. 8a, b, and c. The contact areas were enlarged to make them easier to see. There are two features in common. First, the diameter of the contact area did not noticeably increase with the number of cycles. Second, the characteristics of the lubricating films in the contact area became more and more obvious as the number of cycles increased.

With PAO+NOS (Fig. 8a), at point A₁, where friction was the lowest, slight point-like structures are evident in the contact area. Studies have found that the NOS density increases on the contact surface under boundary lubrication conditions, resulting in a very low friction coefficient [15]. The structures are bigger and more obvious at A₂, where the friction coefficient exceeded that for PAO+ZDDP+NOS. The contact area is similar to the one shown in the companion paper: partially point-like tribo-film formed in the contact area after 5400 sliding cycles. However, as explained in the previous section, the short endurance of the friction reduction performance at room temperature resulted in adsorption density inferior to that at 100°C. According to the EDX results presented in the companion paper, the large structures are reaction products of NOS rich in oxygen. Ravine-like wear scars were observed at A₃. They could have been the physically destroyed tribo-film formed by the NOS. Ravine-like wear scars eventually appeared in the contact area. However, the lubricating oil with added NOS still exhibited good tribological performance as no further increase in the friction coefficient was measured after A₃.

With PAO+ZDDP (Fig. 8b), barely any lubricating film was evident at B₁, where PAO+ZDDP exhibited the lowest friction coefficient. The wear area was scorched yellow with obvious ravine-like structures at B₂, where the friction coefficient was the highest. The color change on the ball and the increase in the

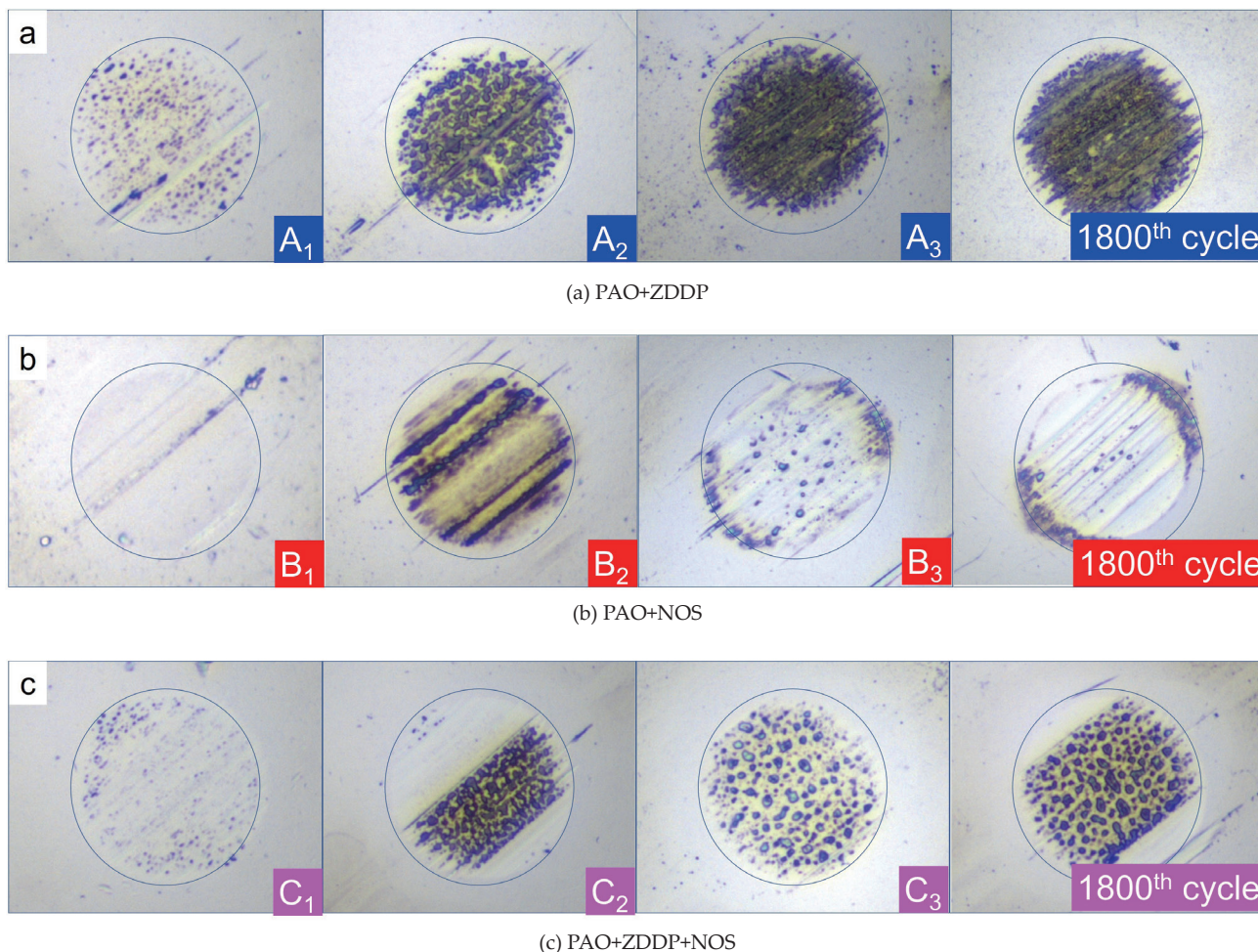


Fig. 8 Wear state of balls when friction coefficient became stable at 5 N

friction coefficient indicates a transition from ZDDP adsorption to ZDDP decomposition under sliding conditions. Then, from B₂ to B₃, the friction coefficient decreased as the tribo-film fully formed. Ravine-like wear scars were evident after the 1800th cycle, which suggests the destruction of the tribo-film under sliding conditions. The ravine-like wear scars may be the reason for the slow increase in the friction coefficient from 600 to 1800 cycles for the ZDDP additive mixtures, as shown in Fig. 3(c).

With PAO+ZDDP+NOS (Fig. 8c), the tribo-film was almost the combination of the tribo-films formed with NOS alone and ZDDP alone. At C₁, the central area exhibited a slight ravine-like feature, similar to that evident at B₁, and the side areas exhibited a point-like feature, similar to that evident at A₁. As the number of cycles increased, points and ravines coupled together and grew gradually from C₂ to C₃. At the 1800th cycle, coupled wear features filled the entire contact area. This suggests that the competitive adsorption of ZDDP and NOS dominates friction behavior during the first 40 cycles. The adsorption of ZDDP limited the friction-reducing ability of NOS, resulting in the highest friction coefficient. The adsorbed NOS suppressed the formation of high-friction ZDDP tribo-film; thus, the increase in the friction coefficient from C₁ was not as sharp as the increase with PAO+ZDDP. In the stabilization stage, NOS continuously inhibited the formation of high-friction tribo-film and inherited the advantages of ZDDP. It thus subsequently exhibited a stable friction coefficient and efficient wear-resistance performance.

With PAO+ZDDP, the friction coefficient and the wear

area increased with ZDDP tribo-film formation. However, the presence of similar point-like structures at A₂, C₂, C₃, and C₄ suggests that ZDDP cannot completely prevent NOS reaction. However, it takes more sliding cycles for NOS in a mixture to form the reaction film (at least 600) than for NOS alone (200). Moreover, the tribo-films formed with PAO+NOS at room temperature differ from those formed at 100°C (shown in the companion paper). This is because NOS can more densely adsorb on metal at 100°C, so tribo-film degradation did not occur during sliding. As a result, point-like structures were not observed in the contact area. Furthermore, ZDDP is more active at higher temperatures, which promotes the formation of ZDDP tribo-film.

3.2 XPS analysis

3.2.1 XPS spectra for tracked area

The XPS spectra of C1s, O1s, Fe2p3, N1s, S2p, and P2p recorded inside the friction track are plotted in Figs. 9a to g. The analyzed area (φ100 μm) was less than the width of the contact area to ensure that the contact area alone was analyzed. This means that the spectroscopic information did not include contributions from the noncontact area. All the signals were fitted using Gaussian/Lorentzian peaks. The binding energies of the photoelectron peaks are listed in Table 3.

C1s spectra. The C1s spectra for all the lubricating oils exhibited the most intense signal at around 285.0 eV, which is assigned to the aliphatic C (C-C, C-H) bond [16]. Minor contributions were found at 286.5 eV, corresponding to

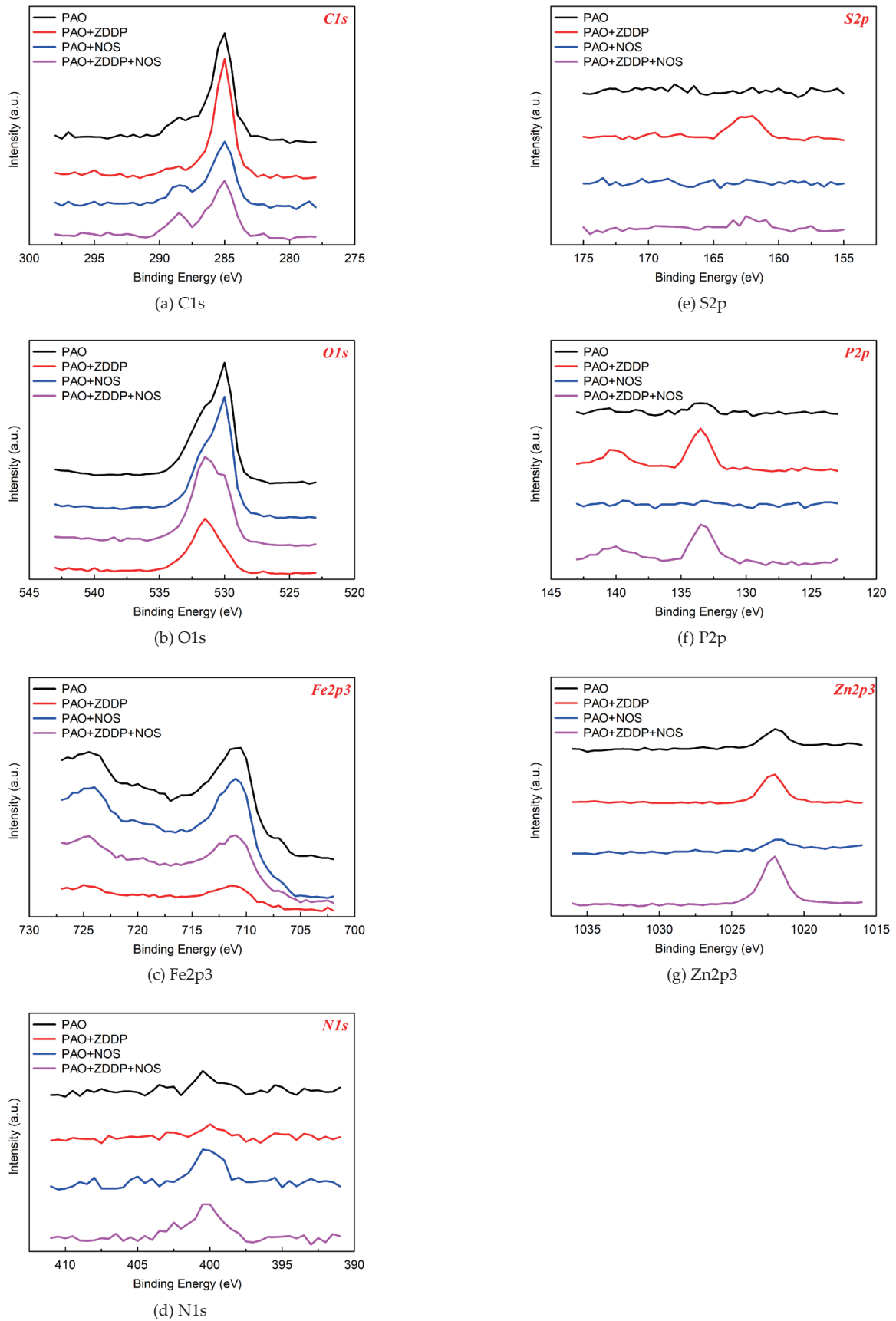


Fig. 9 XPS spectra recorded inside contact areas

Table 3 Binding energies of photoelectron peaks measured in contact areas for reference compounds. Standard deviation is 0.1–0.2 eV for all values listed.

	<i>C1s</i>	<i>O1s</i>	<i>Zn2p3</i>	<i>Fe2p3</i>	<i>P2p</i>	<i>S2p</i>	<i>N1s</i>
PAO	285.1	529.9	1022.0	711.0	—	—	400.2
	286.7	531.4		714.5			
				724.0			
PAO+ZDDP	285.0	531.4	1022.2	711.2	133.5	162.5	—
	286.2	533.8		714.4	140.0		
				724.4			
PAO+NOS	284.9	529.9	1021.8	711.0	—	—	400.1
	286.1	531.2		714.6			
	288.5			724.0			
PAO+ZDDP+NOS	285.0	529.9	1022.0	711.0	133.3	—	400.2
	286.5	531.4		713.9	139.9		
	288.5			724.3			

C-O. As shown in Fig. 10, a third peak around 288.5 eV was recorded for PAO+NOS (Fig. 10a) and PAO+ZDDP+NOS (Fig. 10b); it probably originated from NOS (possibly from its carboxylic groups). This suggests that NOS contributes to tribo-film formation even in an additive mixture. This agrees with the morphology results shown in Fig. 8c: the lubricating film formed by PAO+ZDDP+NOS exhibited synergistic characteristics of PAO+ZDDP and PAO+OS.

O1s spectra. The *O1s* spectra for all the lubricating oils contained two peaks. For PAO, PAO+NOS, and PAO+ZDDP+NOS, there was a common signal peak at around 531.2 eV corresponding to non-bridging oxygen and a minor peak at around 529.9 eV, which may be assigned to Fe-O. The PAO+ZDDP (Fig. 11a) spectra differ completely from those for NOS alone (Fig. 11b) and the NOS+ZDDP mixture (Fig. 11c). With PAO+ZDDP, as shown in Fig. 11a, the signal peaks were at around 531.4 eV and 533.8 eV. The main peak at 531.4 eV can be assigned to the non-bridging oxygen in the poly-phosphate chains and other oxygen-containing groups such as sulphates, carbonates, and hydroxides. [17, 18] The small peak at 533.8 eV is assigned to bridging oxygen [19] in $FePO_4$, which was not detected with PAO+ZDDP+NOS (Fig. 11c). Although the EDX results presented in the companion paper suggest the presence of phosphate, because no PO_4^{3-} signal was recorded with the XPS, the ZDDP does not seem to have completely decomposed in the mixture as the PO_4^{3-} species is one of the final ZDDP decomposition products.

Fe2p3 spectra. The *Fe2p3* spectra for all the lubricating oils could be curve-fitted with three similar signal peaks near 711.0, 714.5, and 724.5 eV, respectively FeO , Fe_2O_3 , and Fe_3O_4 . The most intense signal peak at 711.0 eV is assigned to FeO . However, the intensity of the *Fe2p3* spectra recorded for PAO+ZDDP and PAO+ZDDP+NOS was weaker than for the other mixtures. This suggests that, because the Fe on the friction surface was covered by a thick tribo-film, it was more difficult to detect intense *Fe2p3* spectra. Moreover, with PAO+ZDDP, a thicker lubricating film formed than with PAO+ZDDP+NOS as

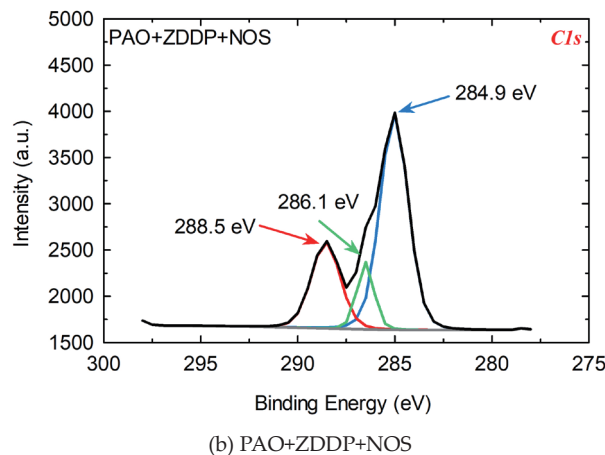
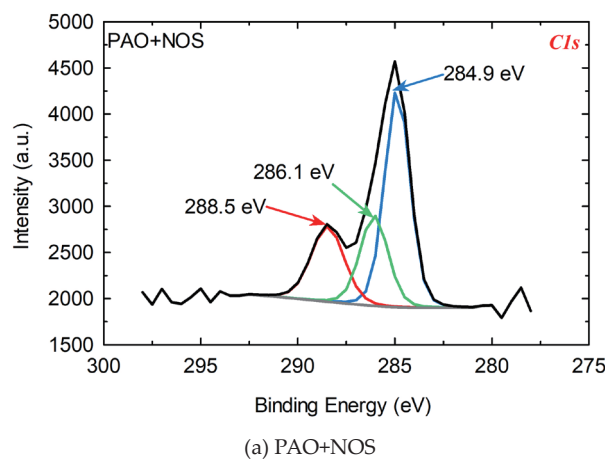


Fig. 10 C1s peak distributions inside contact areas

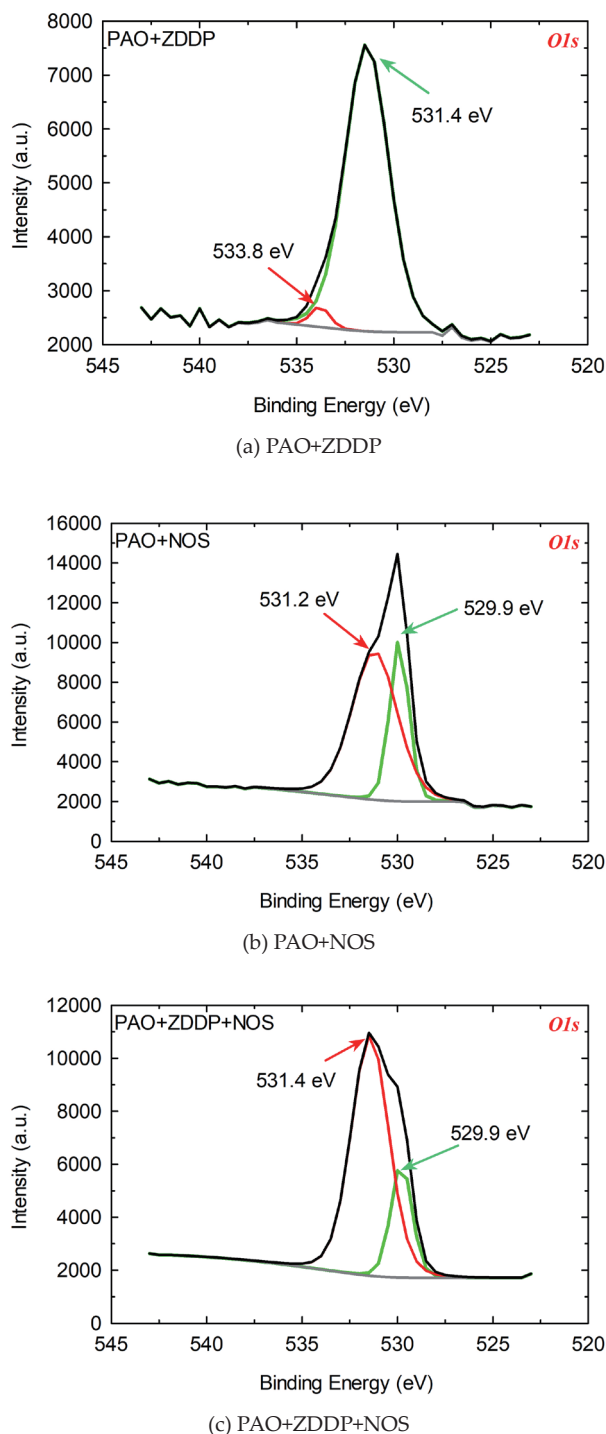


Fig. 11 O1s peak distributions inside contact areas

the weakest intensity was recorded for PAO+ZDDP.

N1s spectra. An intense N1s signal peak at 400.2 eV was recorded for PAO+ZDDP+NOS and PAO+NOS. It originated from the N in the NOS. A very weak N1s signal peak at 400.2 eV was recorded for PAO and PAO+ZDDP. These signals were detected because of the nitriding process in substrate manufacturing. These results agree with the EDX results presented in the companion paper. Nitrogen was detected only on the balls lubricated with NOS alone and the ZDDP+NOS mixture; it was not detected on ones lubricated with PAO and PAO+ZDDP. These results together with those in the

companion paper suggest that NOS strongly adsorbs even in the NOS+ZDDP mixture at both 25 and 100°C.

S2p spectra. The main S2p signal peak was recorded at 162.5 eV only for PAO+ZDDP. The species could be zinc sulfide. Sulfur was also detected for PAO+ZDDP+NOS; however, the peak was not large enough for a proper fit. These results agree with the EDX results presented in the companion paper: the addition of NOS to ZDDP suppressed S formation.

P2p spectra. A P2p signal peak was detected at 133.5 eV for PAO+ZDDP and PAO+ZDDP+NOS. The binding energy at 133.5 eV agrees with the values for phosphate in the literature (133.4–133.8 eV [20, 21]). Another signal peak was detected at 139.9 eV, which originated from Zn3s [16, 19]. This suggests that a Zn-containing lubricating film, possibly a mixture of Zn and P, was formed even when ZDDP was combined with NOS in the lubricating oil. The tribo-film formed by the NOS+ZDDP mixture apparently differs from those formed by an amionic-ZDDP mixture [8, 22], which were rich in Zn and depleted in phosphate. The Zn content was probably zinc oxide induced by the hydrolysis of neutral ZDDP to basic ZDDP caused by the amines [23, 24]. On the other hand, the results for the NOS+ZDDP mixture suggest that no such hydrolysis occurred as the composition of the ZDDP+NOS tribo-film was more similar to the ZDDP tribo-film. The NOS may also prevent the removal of the ZDDP tribo-film resulting from the hydrolysis of neutral ZDDP [10–13].

Zn2p3 spectra. A Zn2p3 signal was detected for all the lubricating oils. A strong signal peak at 1022.0 eV was detected for PAO+ZDDP and PAO+ZDDP+NOS, which can be assigned to Zn sulfide. A weak signal peak was detected at 1022.0 eV for PAO and PAO+NOS. Since these oils did not contain Zn, this signal may have been due to the introduction of trace amounts of Zn during substrate processing, i.e., the wire-cut electrical discharge machining.

3.2.2 XPS spectra outside the contact area

XPS spectra recorded outside the contact area are shown in Fig. 12, and the fitted peak information is listed in Table 4.

The signal distributions for C1s, Fe2p3, and N1s in the noncontact areas were the same as in the contact areas. As shown in Fig. 13, the O1s signals had similar peaks at 529.9 eV and 531.3 eV for PAO+ZDDP (Fig. 13a) and PAO+NOS+ZDDP (Fig. 13b). The peak distribution for PAO+ZDDP differed from that in the contact area. This suggests that tribo-film did not form in the noncontact area. For the NOS+ZDDP mixture, although the peak distribution was the same, the intensity was different. As shown in Fig. 13a, the lower intensity of non-bridging oxygen (poly-phosphate chains, sulphates, carbonates, or hydroxides) around 531.1 eV along with the absence of the O1s signal around 533.8 eV assigned to FePO4 suggests that tribo-film did not form in the noncontact area although molecules of each additive adsorbed on the surface. Another difference between the contact and noncontact areas can be observed in the S2p and P2p signals. First, peaks originating from S2p were not detected in either signal. Second, P2p signals with lower binding energy were detected in both signals; however, the peak values were not large enough for proper fitting. This was because the ZDDP did not decompose into S content and phosphate content as tribo-film was not formed.

From the tribo-film formation discussed in 3.1.2 and the XPS outcomes in 3.2, the mechanism of the anti-wear/friction-reducing performance for PAO+ZDDP+NOS can be inferred as follows: the NOS in the mixture suppresses the formation of

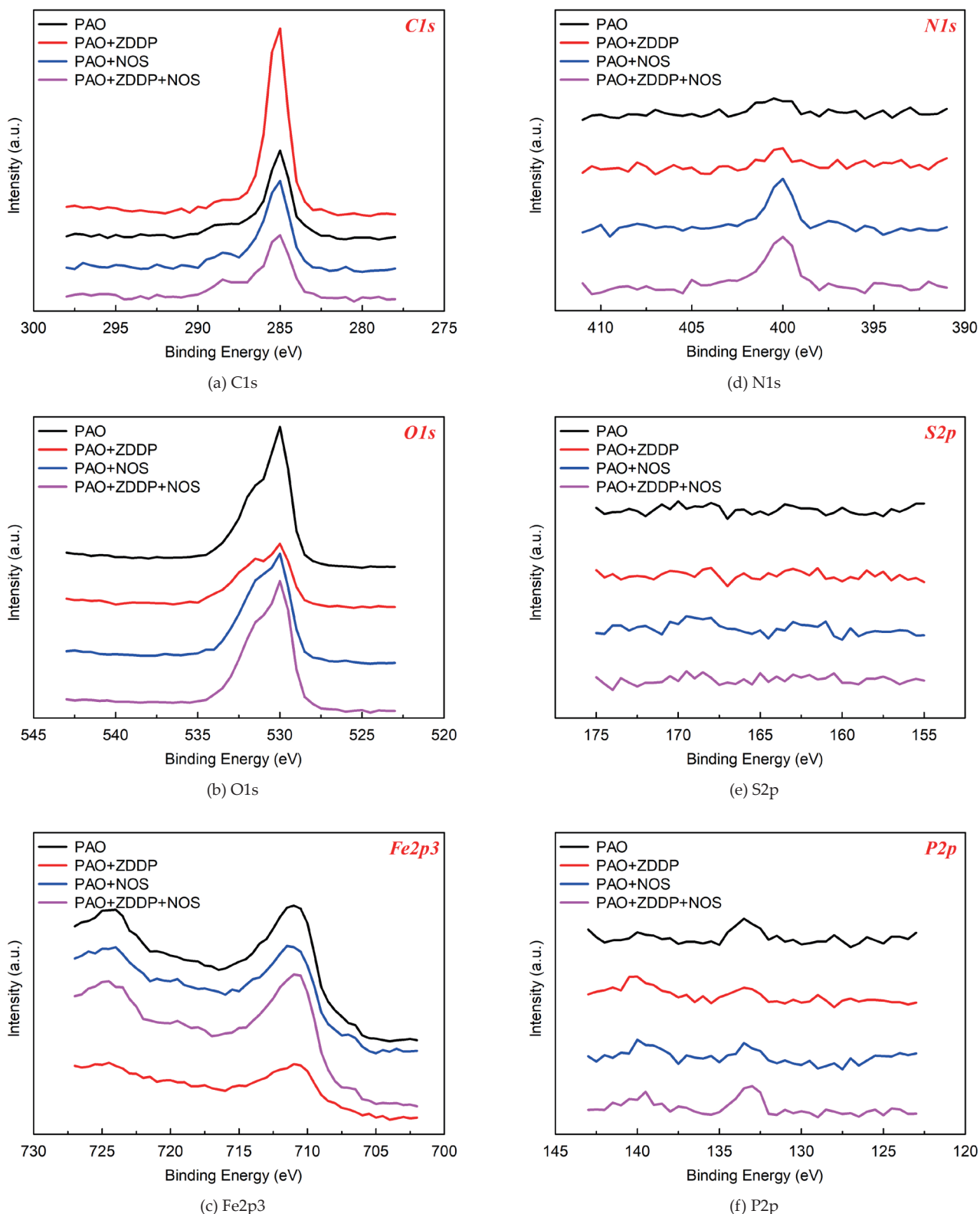


Fig. 12 XPS spectra recorded outside contact areas

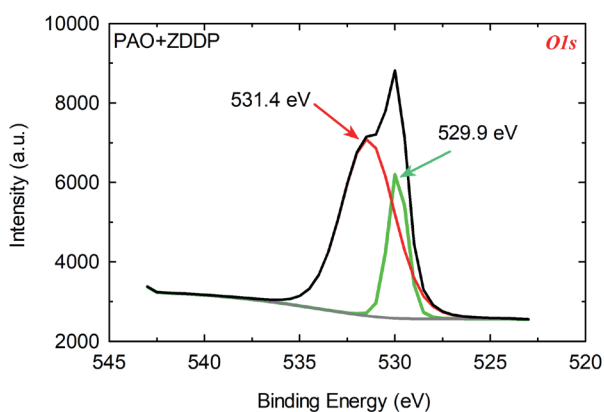
S-containing content in the ZDDP tribo-film, meanwhile, the formation of ZDDP glassy tribo-film retards the degradation of NOS. The tribo-film formed by the mixture inherited both advantages from the tribo-films formed by ZDDP alone and NOS alone but exhibited superior performance to them.

4 Conclusion

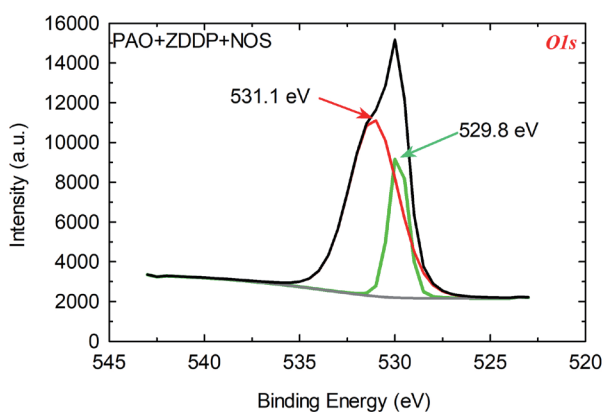
Friction tests, morphological characterization, and surface analyses were performed to clarify the lubricating mechanism of an additive mixture of N-oleoyl sarcosine and zinc dialkyldithiophosphate, focusing on the contribution of the NOS.

Table 4 Binding energies of photoelectron peaks measured outside contact areas for reference compounds. Standard deviation is 0.1–0.2 eV for all values listed.

	C1s	O1s	Zn2p3	Fe2p3	P2p	S2p	N1s
PAO	285.0	529.9	1022.0	711.0	—	—	—
	285.4	531.3		714.8			
				723.9			
PAO+ZDDP	285.1	529.9	1022.0	711.0	—	—	—
	286.2	531.4		714.2			
				724.0			
PAO+NOS	285.1	529.6	—	711.1	—	—	400.2
	286.5	531.1		714.9			
	288.4			724.0			
PAO+ZDDP+NOS	285.1	529.8	1022.0	711.0	—	—	400.2
	286.6	531.1		714.9			
	288.3			724.1			



(a) PAO+ZDDP



(b) PAO+ZDDP+NOS

Fig. 13 O1s peak distributions outside contact areas

- The NOS+ZDDP mixture exhibited enhanced friction-reducing and wear-resistance performance at both 25 and 100°C.

- The film formation process of ZDDP+NOS mixture exhibited the features of both individual additives. Although the friction coefficient was initially high, it decreased and stabilized as the ZDDP tribo-film encased the degraded NOS adsorption film so that the friction-reducing feature of the NOS was maintained.
- Temperature alters the adsorption of NOS and the activeness of ZDDP. NOS adsorbs more densely adsorb on metal at 100°C, prolonging the durability of the adsorption film. In addition, ZDDP is more active at higher temperatures, which promotes the formation of ZDDP tribo-film. However, at both temperatures, with the ZDDP+NOS mixture, NOS degradation does not seem to affect the stability of the tribological behavior.
- Wear diameter was smallest with ZDDP+NOS lubrication under the different loads, suggesting that this mixture has the best load capacity. These results agree well with those presented in the companion paper: the wear diameter of the NOS+ZDDP mixture remained about the same despite increased load and sliding cycles.
- The results of the surface analysis suggest a mechanism for the NOS+ZDDP mixture. First, unlike reported amino-group-containing additives, NOS does not induce the hydrolysis of neutral ZDDP to basic ZDDP. Moreover, NOS probably does not remove the ZDDP tribo-film as other amines do. The NOS and ZDDP competitively adsorb on the metal, causing higher friction during the running-in cycles compared with that with the individual components. Heating enhances NOS adsorption as well as activates ZDDP decomposition. Tribo-film then forms under sliding conditions. However, the NOS prevents the formation of S content and PO_4^{3-} species from the ZDDP. At the same time, the ZDDP prevents NOS degradation. This effect was more remarkable at 100°C because film degradation was not evident, as reported in the companion paper. Eventually, the tribo-film formed with the NOS+ZDDP mixture exhibits synergistic tribological effects under a wide load range regardless of the temperature and sliding time duration.

Acknowledgments

The lubricating oils were provided by ENEOS corporation. The substrate processing was conducted by Mr. HATANO Naoya, technical staff from the Graduate School of Engineering, Kyoto University. This study is financially supported by Grant-in-Aid for Japan Society for the Promotion of Science Fellows (21J15514) and Grant-in-Aid for Scientific Research (A) from the Japan Society for the Promotion of Science (20H00215). Youth Innovation Promotion Association CAS from the Chinese Academy of Sciences (2021141).

References

- [1] Tasdemir, H. A., Wakayama, M., Tokoroyama, T., Kousaka, H., Umehara, N., Mabuchi, Y. and Higuchi, T., "Ultra-Low Friction of Tetrahedral Amorphous Diamond-Like Carbon (ta-C DLC) under Boundary Lubrication in Poly Alpha-Olefin (PAO) with Additives," *Tribology International*, 65, 2013, 286–294.
- [2] Tasdemir, H. A., Wakayama, M., Tokoroyama, T., Kousaka, H., Umehara, N., Mabuchi, Y. and Higuchi, T., "Wear Behaviour of Tetrahedral Amorphous Diamond-Like Carbon (ta-C DLC) in Additive Containing Lubricants," *Wear*, 307, 1–2, 2013, 1–9.
- [3] Taylor, L. J. and Spikes, H. A., "Friction-Enhancing Properties of ZDDP Antiwear Additive: Part I—Friction and Morphology of ZDDP Reaction Films," *Tribology Transactions*, 46, 3, 2003, 303–309.
- [4] Cyriac, F., Yi, T. X., Poornachary, S. K. and Chow, P. S., "Effect of Temperature on Tribological Performance of Organic Friction Modifier and Anti-Wear Additive: Insights from Friction, Surface (ToF-SIMS and EDX) and Wear Analysis," *Tribology International*, 157, 2021, 106896.
- [5] Okubo, H., Watanabe, S., Tadokoro, C. and Sasaki, S., "Effects of Concentration of Zinc Dialkyldithiophosphate on the Tribological Properties of Tetrahedral Amorphous Carbon Films in Presence of Organic Friction Modifiers," *Tribology International*, 94, 2016, 446–457.
- [6] Okubo, H., Tadokoro, C. and Sasaki, S., "Tribological Properties of a Tetrahedral Amorphous Carbon (ta-C) Film under Boundary Lubrication in the Presence of Organic Friction Modifiers and Zinc Dialkyldithiophosphate (ZDDP)," *Wear*, 332–333, 2015, 1293–1302.
- [7] Soltanahmadi, S., Esfahani, E. A., Nedelcu, I., Morina, A., Eijk, M. C. P. and Neville, A., "Surface Reaction Films from Amine-Based Organic Friction Modifiers and Their Influence on Surface Fatigue and Friction," *Tribology Letters*, 67, 3, 2019, 80.
- [8] Massoud, T., De Matos, R. P., Le Mogne, T., Belin, M., Cobian, M., Thiebaut, B., Loehle, S., Dahlem, F. and Minfray, C., "Effect of ZDDP on Lubrication Mechanisms of Linear Fatty Amines under Boundary Lubrication Conditions," *Tribology International*, 141, 2020, 105954.
- [9] Cyriac, F., Yi, T. X., Poornachary, S. K. and Chow, P. S., "Behavior and Interaction of Boundary Lubricating Additives on Steel and DLC-Coated Steel Surfaces," *Tribology International*, 164, 2021, 107199.
- [10] Fujita, H., Glovnea, R. P. and Spikes, H. A., "Study of Zinc Dialkyldithiophosphate Antiwear Film Formation and Removal Processes, Part I: Experimental," *Tribology Transactions*, 48, 4, 2005, 558–566.
- [11] Fujita, H. and Spikes, H. A., "Study of Zinc Dialkyldithiophosphate Antiwear Film Formation and Removal Processes, part II: Kinetic Model," *Tribology Transactions*, 48, 4, 2005, 567–575.
- [12] Miklozic, K. T., Forbus, T. R. and Spikes, H. A., "Performance of Friction Modifiers on ZDDP-Generated Surfaces," *Tribology Transactions*, 50, 3, 2007, 328–335.
- [13] Dawczyk, J., Russo, J. and Spikes, H., "Ethoxylated Amine Friction Modifiers and ZDDP," *Tribology Letters*, 67, 4, 2019, 106.
- [14] Shen, W., Hirayama, T., Yamashita, N., Adachi, M., Oshio, T., Tsuneoka, H., Tagawa, K., Yagishita, K. and Yamada, N. L., "Relationship between Interfacial Adsorption of Additive Molecules and Reduction of Friction Coefficient in the Organic Friction Modifiers-ZDDP Combinations," *Tribology International*, 167, 2022, 107365.
- [15] Ichihashi, T., Kudo, M. and Mori, S., "Relation between the Friction Characteristics of Wet Clutches and the Concentration of Additives Obtained by *In-Situ* Observation of Oil Film," *Journal of Japanese Society of Tribologists*, 58, 8, 2013, 581–588 (in Japanese).
- [16] Nedelcu, I., Piras, E., Rossi, A. and Pasaribu, H. R., "XPS Analysis on the Influence of Water on the Evolution of Zinc Dialkyldithiophosphate-Derived Reaction Layer in Lubricated Rolling Contacts," *Surface and Interface Analysis*, 44, 8, 2012, 1219–1224.
- [17] Heuberger, R., Rossi, A. and Spencer, N. D., "XPS Study of the Influence of Temperature on ZnDTP Tribofilm Composition," *Tribology Letters*, 25, 3, 2007, 185–196.
- [18] Rossi, A., Piras, F. M., Kim, D., Gellman, A. J. and Spencer, N. D., "Surface Reactivity of Tributyl Thiophosphate: Effects of Temperature and Mechanical Stress," *Tribology Letters*, 23, 3, 2006, 197–208.
- [19] Crobu, M., Rossi, A., Mangolini, F. and Spencer, N. D., "Chain-Length-Identification Strategy in Zinc Polyphosphate Glasses by Means of XPS and ToF-SIMS," *Analytical and Bioanalytical Chemistry*, 403, 5, 2012, 1415–1432.
- [20] Piras, F. M., Rossi, A. and Spencer, N. D., "Combined *In Situ* (ATR FT-IR) and *Ex Situ* (XPS) Study of the ZnDTP-Iron Surface Interaction," *Tribology Letters*, 15, 3, 2003, 181–191.
- [21] Schuetzle, D., Carter, R. O., Shyu, J., Dickie, R. A., Holubka, J. and McIntyre, N. S., "The Chemical Interaction of Organic Materials with Metal Substrates. Part I: Esca Studies of Organic Phosphate Films on Steel," *Applied Spectroscopy*, 40, 5, 1986, 641–649.
- [22] Matsui, Y., Aoki, S. and Masuko, M., "Influence of Coexisting Functionalized Polyalkylmethacrylates on the Formation of ZnDTP-Derived Tribofilm," *Tribology International*, 100, 2016, 152–161.
- [23] Harrison, P. G., Begley, M. J., Kikabhai, T. and Killer, F., "Zinc(II) Bis(O,O'-Dialkyl Dithiophosphates): Interaction with Small Nitrogen Bases. The Crystal and Molecular Structure of Hexakis(μ -O,O'-Diethyl Dithiophosphato)- μ -4-Thio-Tetrazinc, Zn₄[S₂P(OEt)₂]₆S," *Journal of the Chemical Society, Dalton Transactions*, 5, 1986, 925–928.
- [24] Yamaguchi, E. S., Onopchenko, A., Francisco, M. M. and Chan, C. Y., "The Relative Oxidation Inhibition Performance of Some Neutral and Basic Zinc Dithiophosphate Salts," *Tribology Transactions*, 42, 4, 1999, 895–901.



This paper is licensed under the Creative Commons Attribution-NonCommercial-NoDerivatives 4.0 International (CC BY-NC-ND 4.0) License. This allows users to copy and distribute the paper, only upon conditions that (i) users do not copy or distribute such paper for commercial purposes, (ii) users do not change, modify or edit such paper in any way, (iii) users give appropriate credit (with a link to the formal publication through the relevant DOI (Digital Object Identifier)) and provide a link to this license, and (iv) users acknowledge and agree that users and their use of such paper are not connected with, or sponsored, endorsed, or granted official status by the Licensor (i.e. Japanese Society of Tribologists). To view this license, go to <https://creativecommons.org/licenses/by-nc-nd/4.0/>. Be noted that the third-party materials in this article are not included in the Creative Commons license, if indicated on the material's credit line. The users must obtain the permission of the copyright holder and use the third-party materials in accordance with the rule specified by the copyright holder.